chemistry

MDPI

Article

Nature Inspired Manganese(III)-Calcium Complexes: Towards Synthetic Models for the WOC of PSII

Joaquin Bonelli Blasco [1], Sara Mauri Querol [1], Kevin Consuegra Naranjo [1] and E. Carolina Sañudo [1,2,*]

[1] Departament de Química Inorgànica i Orgànica, Facultat de Química, Universitat de Barcelona, C/Martí i Franqués 1-11, 08028 Barcelona, Spain
[2] IN2UB Institut de Nanociència i Nanotecnologia, Universitat de Barcelona, C/Martí i Franqués 1-11, 08028 Barcelona, Spain
* Correspondence: esanudo@ub.edu

Abstract: For some time, the presence of high oxidation state Mn ions and Ca(II) in the active center of Photosystem II has been known. However, coordination complexes that combine both Mn(III) and Ca(II) have been difficult to obtain, with only a handful of examples reported. In this paper we report the synthesis of two new Mn(III)-Ca(II) complexes, **1** $[Pr_2NH_2]_3[Mn_6CaO_2(OH)(OMe)_3(SALO)_6(SALOH)_3]$ and **2** $[Mn_{18}Ca_6O_{12}(OH)_6(MeO)_{12}(PhCOO)_{18}(MeOH)_6]$. The complexes have been characterized by single-crystal X-ray diffraction to establish the oxidation state of manganese. The use of salicylato ligands with tert-butyl substituents leads to effective encapsulation of a Ca(II) ion in a cavity that has both hydrophobic and hydrophilic regions, mimicking the enzyme environment.

Keywords: WOC; manganese(III)-calcium(II); PSII

Citation: Bonelli Blasco, J.; Mauir Querol, S.; Consuegra Naranjo, K.; Sañudo, E.C. Nature Inspired Manganese(III)-Calcium Complexes: Towards Synthetic Models for the WOC of PSII. *Chemistry* **2023**, *5*, 703–712. https://doi.org/10.3390/chemistry5020049

Academic Editors: Zoi Lada and Konstantis Konidaris

Received: 28 February 2023
Revised: 13 March 2023
Accepted: 21 March 2023
Published: 23 March 2023

1. Introduction

Photosystem II (PSII) is the membrane protein in plants and cyanobacteria that is responsible for aerobic life on Earth. The PSII active center is known as the water oxidation center (WOC) or oxygen-evolving complex (OEC), and it oxidizes water to O_2, releasing this oxygen to the atmosphere. The oxidation of water involves proton-coupled multi-electron transfers (PCET) in a very complex active site the structure of which has remained elusive for a long time. Various techniques showed that the active site contained manganese ions, but it was not until 2011 that a 1.9 Å resolution crystal structure showed without ambiguity that the active site was formed by a Mn_4CaO_5 active center [1]. The WOC is thus formed by a Mn_3Ca +Mn or cubane + monomer structure, that cycles in several oxidation or S states (Kok's cycle) to produce O_2. In 2014 authors showed by XFEL experiments a "radiation damage free" structure, confirming the observed Mn_4CaO_5 active center and the oxidation states of the Mn ions tentatively assigned to two Mn(III) and two Mn(IV) [2,3]. Bond distance and Jahn–Teller distortions on the Mn centers were used to assign the tentative oxidation states, which had been previously considered to be Mn(III).

In 2014, a review on manganese/calcium complexes [4] revealed only twenty examples of complexes and four coordination polymers that combined manganese and calcium. In many of the reported cases manganese was in an oxidation state (II), and only a few contained Mn(III). The motif Mn_3Ca cubane was found in some of the examples, even though the water oxidation function of PSII was never demonstrated. Few examples have been reported after, including an $Mn(III)_2Ca_2$ complex reported in 2017 with single-molecule magnets (SMM) properties [5]. The seminal work on Mn(III)/Ca complexes was completed by Agapie who reported $Mn(III)_3Ca$ complexes from 2011, with the Mn_3Ca cubane structural motif [6–8]. In 2012, Christou and coworkers reported an $Mn(IV)_3Ca$ cubane complex, with pivalate ligands [9]. In 2015, a Mn_4Ca complex was reported with the cubane monomer structure [10]. Despite the successes in synthetically reproducing the

structure of WOC and showing how the monomer Mn ion affects the redox potential of the other three Mn in the Mn_4Ca unit, reproducing the water oxidation function to photocatallitically generate oxygen from water has not been possible. It has been clear for a time that the secondary coordination sphere of the WOC plays an important role in maintaining the complex structure through Kok's cycle, and that it also has an important role to promote PCET reactions. Mimicking the protein envelope of WOC in PSII is an amazing challenge for coordination chemists. The environment of the metal oxide core must have both polar and non-polar sites. This can be completed by ligand design. In particular, substituted salicylato ligands have an OH group in ortho to a carboxylic acid group in a phenyl ring. Substitutions of the 3,5-H of the phenyl ring are easily obtained. Thus, substituted salicylato ligands are amenable to producing such a combination of polar and non-polar sites if the substituents of the phenyl group are carefully chosen.

We had worked in the past with salicylato ligands with a variety of groups in the 3,5-C of the phenyl ring. When the substituents are tert-butyl groups, we reported an Mn_7 complex [11], and later a family of Mn(III)-Ln(III) complexes [12]. The Mn_6M' species reported share the same core, with different central ions, which can be Mn(II) for Mn_7 or a lanthanoid ion for Mn_6Ln. Given the low number of high-oxidation manganese/calcium complexes reported in the literature, we found it interesting to attempt to modify our previously reported Mn_6Ln complexes [12] to obtain Mn(III)-Ca complexes. The ionic radii for the lanthanoid ions are between 117 pm for La(III) to 105 pm for Dy(III), very similar to 114 pm for Ca(II). The Mn_6 moiety encapsulates an Ln(III) ion in these complexes, so it should be able to also encapsulate a Ca(II) ion. We followed our reported synthetic procedure to synthesize Mn(III) complexes with Ca(II), the results are reported herein.

2. Materials and Methods

All chemicals and solvents were obtained from commercial sources (metal salts from Sigma-Aldrich, organic ligands from Sigma-Aldrich and TCI Europe; all solvents were obtained from Sigma-Aldrich) and used as received, without further purification. All chemicals used in the syntheses are reagent grade.

$[Pr_2NH_2]_3[Mn_6CaO_2(OH)(OMe)_3(SALO)_6(SALOH)_3]$ (complex 1):

Dipropylamine (0.278 mL; 1.0107 mmol) is added to a mixture of $MnCl_2{\cdot}4H_2O$ (0.100 g, 0.505 mmol), $Ca(NO_3)_2{\cdot}4H_2O$ (0.0199 g, 0.08422 mmol and 3,5- di-tertbutylsalicylic acid (0.253 g; 1.0107 mmol) in MeCN (8 mL) and MeOH (2 mL). The resulting dark green solution is stirred for 10 min until the total dissolution of all reagents. After 3 days brown crystals appear. The crystals are dissolved in MeOH:MeCN (1:4 ratio) and one equivalent of $TBAMnO_4$ is added with excess dipropylamine. Brown–green crystals grow from slow evaporation of the solvent, in 2% yield.

Theoretical elemental analysis (experimental) of $1{\cdot}2H_2O$: C 60.57 (60.13), H 7.99 (7.81), N 1.33 (1.41) %. Selected IR data (cm−1): 3416.99 (w), 2903.17 (w), 2867.34 (w), 1611.54 (w), 1550.98 (m-s), 1439.88 (m-s).

$[Mn_{18}Ca_6O_{12}(OH)_6(MeO)_{12}(PhCOO)_{18}(MeOH)_6]$ (complex 2):

Dipropylamine (0.416 mL; 3.032 mmol) is added to a mixture of $MnCl_2{\cdot}4H_2O$ (0.100 g, 0.505 mmol), $Ca(NO_3)_2{\cdot}4H_2O$ (0.00312 g, 0.126 mmol), benzoic acid (0.128 g; 1.011 mmol) in MeCN (8 mL) and MeOH (2 mL). The resulting dark brown solution is stirred for 10 min until the total dissolution of all reagents. After 15 days brown crystals appear which are suitable for X-ray diffraction. Yield < 5%.

Selected IR data (cm^{-1}): 3415.63 (m), 3057.76 (w), 2962.32 (w), 2925.36 (w), 1600.82 (s), 1553.33 (s), 1401.96 (s).

$[Pr_2NH_2]_3[Mn(Cl_2SALO)_3]$ (complex 3):

Dipropylamine (0.278 mL; 1.0107 mmol) is added to a mixture of $MnCl_2{\cdot}4H_2O$ (0.100 g, 0.505 mmol), $Ca(NO_3)_2{\cdot}4H_2O$ (0.0199 g, 0.08422 mmol and 3,5- dichlorosalicylic acid (0.253 g; 1.0107 mmol) in MeCN (8 mL) and MeOH (2 mL). The resulting dark green solution is stirred for 10 min until the total dissolution of all reagents. After 3 days, brown crystals appear that are identified as complex 3 by single-crystal X-ray crystallography. Yield 10%.

Characterization

Infrared spectra have been collected on KBr pellets on a Thermo Nicolet AVATAR 330 FT-IR at Departament de Quimica Inorgànica, Universitat de Barcelona. X-ray diffractions have been collected on a Bruker APEXII SMART diffractometer using molybdenum Kα microfocus (λ = 0.71073 Å). Magnetic measurements were performed at the Unitat de Mesures Magnètiques of the Universitat de Barcelona on a Quantum Design SQUID MPMS-XL magnetometer equipped with a 5 T magnet. Diamagnetic corrections for the sample holder and for the sample using Pascal's constants were applied. XPS spectra were collected at CCiTUB.

3. Results

3.1. Synthesis and Crystal Structures

For a time, we have exploited the coordination chemistry of substituted salicylato ligands as those shown in Scheme 1. The R1 and R2 groups that we have used for this work and the tert-butyl groups. These aliphatic substituents provide the compounds with greater solubility in a common organic solvent, at the same time that they provide an aliphatic, non-polar hydrophobic envelope to the Mn oxide core. This is nicely combined with the phenol group of the salicylato ligand, which provides a possible H-bonding unit and a hydrophilic site in an otherwise very hydrophobic molecule. Combining these properties, we have been able to achieve a series of new structural types in Mn oxide chemistry [11,13]. In particular, we were able to obtain a series of Mn_6Ln complexes with a central Ln(III) ion of formula $[Pr_2NH_2]_3[Mn_6LnO_3(OMe)_3(SALO)_6(SALOH)_3]$ (Ln = La, Tb, Gd, Dy) [12]. The ionic radii similarity between the lanthanoid ions and Ca(II) should facilitate the placement of a Ca(II) ion in the coordination pocket occupied by the lanthanoid ions. At the same time, the compounds produced should be able to mimic the combination of polar and non-polar environments found in enzymes. We used calcium nitrate and manganese(II) chloride in a 1:4 ratio expecting to obtain a similar complex with four Mn(III) and one Ca(II), however, we obtained a compound with a similar core to our reported Mn_6Ln. The crystals of these species diffracted always too poorly, and we were not able to obtain a good quality crystal structure. R_{int} values were always of the order of 15–25%, thus no meaningful chemical formula or bond distances could be extracted from these results. However, we were able to establish a Mn_6Ca core for these species, this encouraged us to further explore this reaction system. We decided to oxidize this material with $TBAMnO_4$. From the reaction with $TBAMnO_4$ we were able to obtain a crystal that could be analyzed by single-crystal X-ray crystallography as complex **1**, $[Pr_2NH_2]_3[Mn_6CaO_2(OH)(OMe)_3(SALO)_6(SALOH)_3]$.

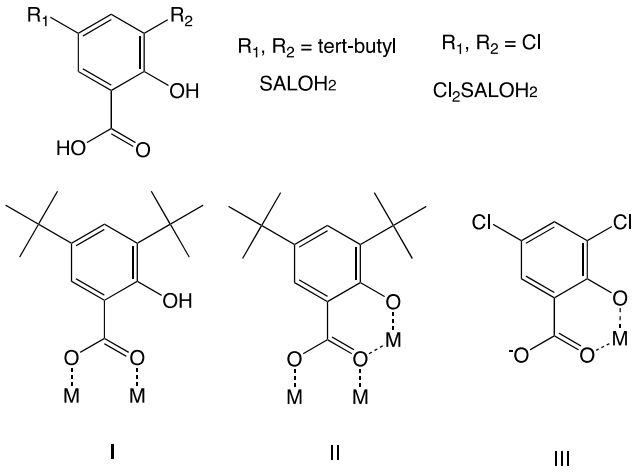

Scheme 1. Salicylato ligands used in this work with their binding modes.

It is clear that the OH group of $SALOH_2$ ligand is not innocent, since it plays a major role in bridging the metal ions in complex **1**, and it serves to provide a hydrophilic binding site in the complex. This is in line with the observations of the role of the secondary coordination sphere in WOC reactivity. In our last attempt to modify the chemical reaction that leads to complex **1**, we tackled carboxylic acid. In one set of reactions, we replaced the tert-butyl and OH groups with protons, using benzoic acid. In the second set of reactions, we replaced the tert-butyl groups with chlorine atoms, using Cl_2SALOH_2.

When benzoic acid was used instead of $SALOH_2$, we isolated complex **2**. Complex **2** contains eighteen manganese ions and six calcium(II) ions. A similar complex had been reported in the literature, with Cu(II) ions instead of Ca(II) [14].

The results indicated that the OH group of the salicylate ligand along with the substituents is necessary, so we decided to change the nature of the other substituents. When Cl_2SALOH_2 is used instead of $SALOH_2$, we isolated complex **3**. Complex **3** is a simple monomer with three Cl_2SALO ligands and three dipropylammonium counterions.

The reactions are shown in reaction Scheme 2.

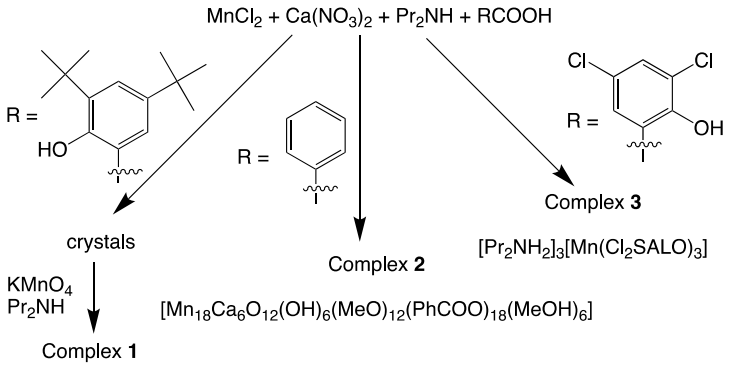

Scheme 2. Reaction scheme for the complexes **1**, **2** and **3** presented here.

XPS analyses were performed for both **1** and **2** to confirm the presence of Ca(II) and Mn. Quantification of the Mn and the Ca 2p regions gives approximate atomic ratios of Mn:Ca of 6:1 for **1** and 3:1 for **2**, in agreement with the expected formulae. XPS spectra are found in ESI Figures S1 and S2.

The crystal structure and data collection parameters for **1–3** are listed in ESI Table S1. Complex **1** crystallizes in the trigonal space group R3-. Figure 1 shows the crystal structure

and the core of complex **1**. The asymmetric unit contains two Mn ions, 1/3 of the Ca(II) ion, and the relevant ligands. The core of the complex is formed by three dinuclear Mn_2 units, generated by the symmetry operations of the trigonal space group. In each Mn_2 unit, the two Mn ions are bridged by a MeO-, one oxygen, and a SALOH ligand using its COO- group in the typical syn–syn bridging mode (coordination type I in Scheme 1). The bridging oxygen is bridging the two Mn ions in the dimer to the central Ca(II). The six SALO ligands link one Mn of each dimer to the central Ca(II), using the deprotonated phenol to bind to the Mn and the carboxylato group in a syn–syn, anti-bridging mode to coordinate the Ca(II) to two Mn ions of two Mn_2 units (coordination type II in Scheme 1). The Mn2 unit is formed by Mn1 and Mn2. The oxidation state of the Mn ions and the protonation state of the ligands were established by bond valence sum calculations [15–17]. Full BVS tables can be found in ESI Table S2. Mn1 has a clear Jahn–Teller elongation, with two trans distances of 2.353 Å and 2.087 Å, while the average of the other four Mn-O distances is 1.91 Å. BVS calculations give BVS values of Mn(II): 3.33; Mn(III): 3.05; Mn(IV): 3.20, so the oxidation state of Mn1 can be unambiguously assigned as Mn(III). Mn2 does not show a clear Jahn–Teller distortion, with three distances above 2 Å and three around 1.9 Å. Furthermore, one of the SALO ligands coordinated to Mn2 is crystallographically disordered in two positions. Thus, there are two sets of Mn2-O distances, one for disorder part A and one for disorder part B. The average BVS values for both parts are Mn(II): 3.38; Mn(III): 3.10; Mn(IV): 3.25. Mn2 generates the symmetry-related Mn2′ and Mn2′′. The BVS values indicate that the oxidation states for Mn2, Mn2′, and Mn2′′ is Mn(III). The BVs of O1 and O2 give values of 1.28 for O2, a typical value for a deprotonated MeO- ligand bridging two Mn ions. However, the BVS value for O1, the mononuclear μ_3-oxygen is 1.75. This value should be 2 for an oxido ligand, but as in this structure O2 generates the symmetry-related O2′ and O2′′, it is necessary for charge balance that one oxygen is a μ_3-OH- ligand. This yields the formula $[Pr_2NH_2]_3[Mn_6CaO_2(OH)(OMe)_3(SALO)_6(SALOH)_3]$ for complex **1**. The three ammonium counterions are hydrogen bonding to two oxygen atoms from two Mn2 units, with d(N-O1) = 2.760 Å and d(N-O2) = 2.644 Å.

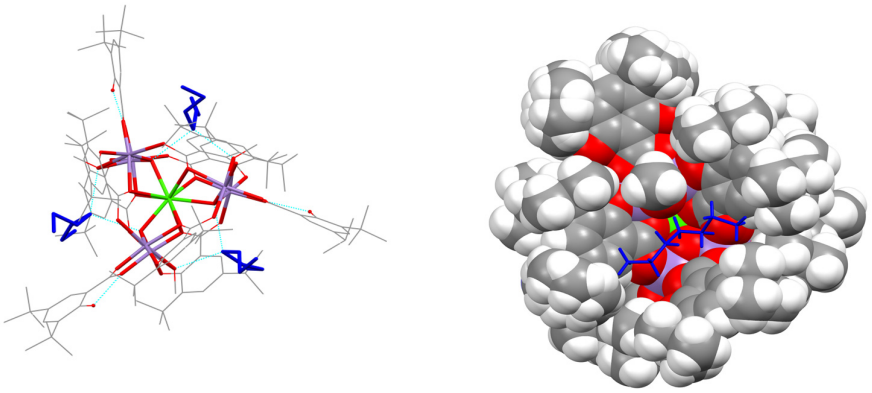

Figure 1. Crystal structure of complex **1**, the Mn_6Ca-oxido core is shown as capped sticks, while the carbon atoms on ligands are shown in wireframe style for clarity. The three dipropylammonium counterions are shown in blue and H-bonding interactions are in cyan. H atoms omitted for clarity in the stick representation of complex **1**. C: grey; O: red; N: blue; Mn: purple; Ca: green. The right view shows a space-fill view of the cavities where the dipropylammonium cations (in blue-capped sticks) sit.

Complex **2** crystallizes in trigonal space group P3-. Figure 2 shows the crystal structure of **2**. Complex **2** has a $[Mn(III)_{12}O_{12}]$ core with twelve Mn(III) cations and the twelve O^{2-} anions forming a hollow cube, as shown in Figure 3. There are six Mn(II) ions around the $[Mn(III)_{12}O_{12}]$ core, and six Ca(II) surround the Mn/O core. All Mn(II) and Mn(III) are hexacoordinated, with a clear Jahn–Teller effect on the Mn(III) ions. BVS calculations

confirm the assigned oxidation states. Full BVS tables can be found in ESI Table S2. The calcium ions are heptacoordinated.

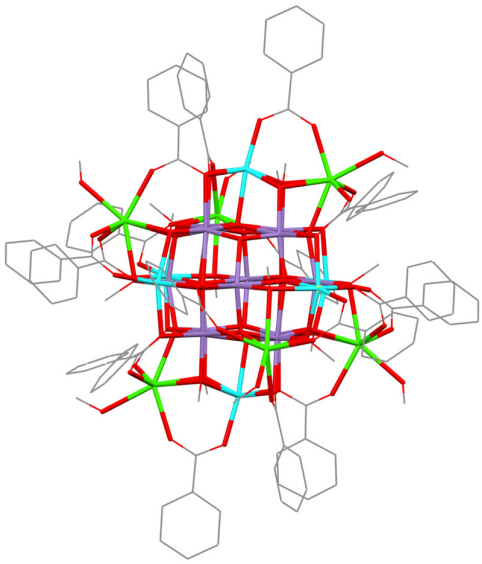

Figure 2. Crystal structure of complex **2**, the MnCa-oxido core is shown as capped sticks, while the carbon atoms on ligands are shown in wireframe style for clarity. H atoms omitted for clarity. C: grey; O: red; N: blue; Mn(III): purple; Mn(II): cyan; Ca: green.

The crystal structure of complex **3** is shown in Figure 3. Complex **3** crystallizes in the orthorhombic space group Pbca. It is a mononuclear Mn(III) complex, with three Cl_2SALO ligands. The Mn ion is in oxidation state Mn(III) and it shows a clear Jahn–Teller elongation. Two trans Mn-O distances are 2.167 Å and 2.217 Å, while the average Mn-O distance in the equatorial plane of the octahedral coordination sphere is 1.917 Å. The three Cl_2SALO ligands are completely deprotonated and coordinate the Mn(III) ion in the unusual binding mode III in Scheme 1. For charge balance, there are three dipropylammonium cations in the asymmetric unit.

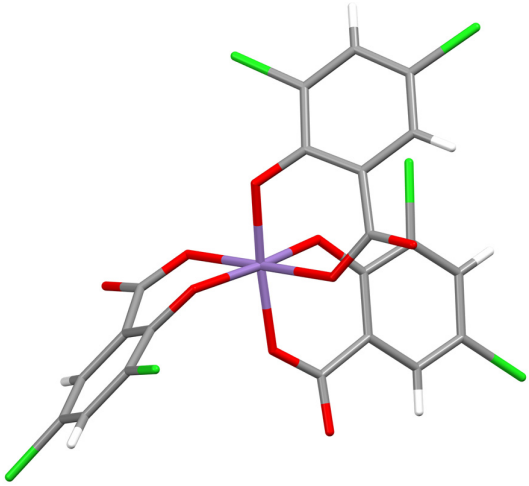

Figure 3. Crystal structure of the anion of compound **3**. C: grey; H: light grey; O: red; N: blue; Mn(III): purple; Cl: green.

3.2. Magnetic Properties

Dc magnetic susceptibility was collected for complexes **1** and **2** in a commercial SQUID with an applied DC field of 5000 Oe in the 2 to 300 K temperature range.

Magnetization vs. field data were collected at 2 K in the 0 to 5 T magnetic field range.

The χT vs. T plot for complex **1** shows a χT product value at 300 K of 18.45 emu K/mol, slightly above the expected value of 18 emu K/mol for six independent Mn(III) ions with S = 2 and g = 2.0. As temperature decreases, the χT product increases to a value of 21.34 emu K/mol at 45 K, and then it gradually decreases to a value of 6 emu K/mol at 2 K. The magnetic behavior of **1** is analogous to the magnetic properties of Mn_6La, as expected since the oxidation state of the Mn(III) ions is the same and the coordination environment and geometries are very similar [12]. The susceptibility data were fitted using PHI [18] to a model of three independent $Mn(III)_2$ units. This is a very simple model that includes the coupling between the $Mn(III)_2$ units as zJ′ term. The dinuclear units are bridged by *syn,anti*-carboxylato groups and magnetic exchange could be mediated by the diamagnetic Ca(II) central ion. The values used to model the experimental data were J = +5.0 cm^{-1}, and the single-ion anisotropy was reflected in a second-rank Stevens operator of |11.0| cm^{-1}, with g = 1.97; this is shown in Figure 4 as a solid line.

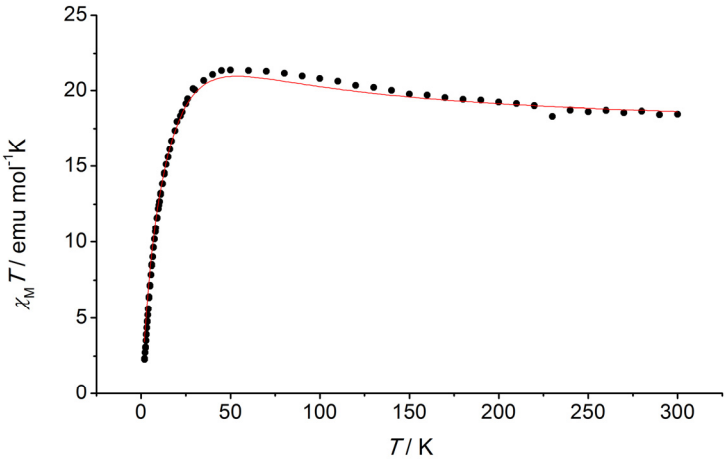

Figure 4. Magnetic data for complex **1**, showing a χT vs. T plot collected at 5000 G and the best fitting of the experimental data as a solid line (see text for fitting parameters).

Magnetic data for complex **2** are shown in Figure 5. The χT vs. T plot for complex **2** shows a continuous decrease in the χT product from a value of 61.78 emu K/mol at 300 K to a value of 8.5 emu K /mol at 2 K due to antiferromagnetic coupling. The χT value at room temperature is slightly below the expected value of 62.25 emu K/mol for 12 Mn(III) and 6 Mn(II) independent ions. The magnetization vs. field plot at 2K shows a monotonous increase in the $M/N\mu_B$ value from zero to a value of 17 at 5 T. This indicates the population of a manifold of excited states that are easily accessible at 2 K.

Figure 5. Magnetic data for complex **2**, showing a χT vs. T plot collected at 5000 G and magnetization vs. field plot at 2 K.

Ac magnetic susceptibility data were collected at various fields and ac frequencies, in the absence of a dc magnetic field, and at various dc magnetic fields. There was no evidence of slow relaxation of the magnetization for either **1** or **2**.

4. Discussion

We report here two new Mn(III)-Ca(II) complexes of formulae **1** $[Pr_2NH_2]_3[Mn_6CaO_2(OH)(OMe)_3(SALO)_6(SALOH)_3]$ and **2** $[Mn_{18}Ca_6O_{12}(OH)_6(MeO)_{12}(PhCOO)_{18}(MeOH)_6]$. XPS data confirms that Ca(II) is present in both **1** and **2**. This is particularly relevant for complex **1** since a similar compound with Mn in the central position is known [11]. The Mn oxidation states in both complexes (Mn(III) in **1** and a mixture of Mn(II) and Mn(II) in **2**) are established by BVS using the single crystal data, and they are confirmed by the magnetic data.

The tert-butyl groups in the SALO ligands present in complex **1** provide a mock-protein environment, where OH- groups coexist with very hydrophobic residues. This does not happen in complex **2**, with benzoato ligands, or when the tert-butyl groups are substituted by chlorine atoms, like in complex **3**.

The tert-butyl substituted SALO ligands provide an external hydrophobic surface to complex **1**, while hydrophilic cavities are defined by O1 and O2, the OH groups of SALOH ligands also contribute to this combination of hydrophilic parts and a hydrophobic surface. The three dipropylammonium counterions sit in these cavities, with the polar NH_2^+ group close to the Mn_6Ca oxide core and the aliphatic tails pointing outwards, towards the tert-butyl substituents, as shown in Figure 1. The more polar cavity of complex **1** encapsulates Ca(II). Although further work should still be completed in order to obtain better models of WOC in PSII, the structure of complex **1** is promising and it opens up synthetic possibilities. The calcium atom in complex **1** is located in an interesting position because, with three of the manganese that surrounds it, it can be a precursor of the distorted cubane of the cluster of WOC. Distances between calcium and manganese atoms that are inside the cubane in WOC are 3.3–3.5 Å [2,3], which is a similar value to the 3.404 and 3.407 Å Mn-Ca distances in complex **1**. The other Ca-Mn distance in the cluster of WOC (distance between calcium and "dangler" manganese) is 3.8 Å, a similar value is not found in complex **1**. Post-synthetic modifications to complex **1** might in the future yield better models for WOC in PSII.

The use of ligands without tert-butyl groups, or the ortho OH- group of SALO results in different species obtained. Complex **2**, with benzoato ligands, contains both Mn(III) and Ca(II), but it also contains Mn(II). Complex **3**, however, is a monomeric species and does not contain Ca(II). This shows the importance of ligand design for biomimetic complexes. The protein environment found in enzymes such as PSII provides a unique envelope that has hydrophobic and polar pockets. In order to prepare synthetic analogs to the active sites of enzymes, this is a crucial feature that a ligand set must possess. However, as evidenced in complexes **1**, **2,** and **3**, this is not all that is needed. A systematic approach to ligand design and to heteroleptic systems is necessary to achieve synthetic analogs of the

active sites of enzymes. In particular, in the system presented here, the SALO ligand provides access to complex **1**.

5. Conclusions

In this work, we have shown how a tert-butyl substituted salicylato ligand can be used to mimic nature and create coordination complexes with polar and non-polar sites. In this paper we report the new Mn(III)-Ca(II) complexes of formulae **1** $[Pr_2NH_2]_3[Mn_6CaO_2(OH)(OMe)_3(SALO)_6(SALOH)_3]$ and **2** $[Mn_{18}Ca_6O_{12}(OH)_6(MeO)_{12}(PhCOO)_{18}(MeOH)_6]$. The complexes have been characterized by single-crystal X-ray diffraction, XPS, IR, and magnetic measurements. The combination of the data obtained has served to ascertain the oxidation state Mn(III) for all Mn ions in **1** and for 12 of the 18 Mn ions in **2**. We thus report a viable reaction system to obtain Mn(III)-Ca(II) complexes. Such species are relevant as synthetic models to the active site of the enzyme Photosystem II, in the literature only a handful of complexes that contain both Mn(III) and Ca(II) have been reported. From the species we report here, we want to emphasize that the use of suitable ligands such as the tert-butyl substituted SALO are of utmost importance in the challenge to obtain synthetic analogs to the WOC of PSII. As we show, the use of simple ligands such as benzoato or ligands that lack the duality polar/apolar sites of SALOH such as the dichloro analog used here to obtain complex **3** do not achieve coordination complexes that can be useful for the preparation of synthetic analogs to active sites in enzymes. Furthermore, we believe that the study of heteroleptic Mn/Ca systems that combine ligands such as SALO and others will be key to attaining suitable synthetic models for WOC in PSII. To model the environment of the enzyme, it is necessary to have ligands that mimic the protein environment so that they can provide apolar pockets combined with polar sites. As we show here, highly symmetric complexes are obtained from homoleptic reaction systems, thus heteroleptic systems must be explored. Complex **1** can be a great synthetic platform, as it can be used as a Mn_6Ca starting material for heteroleptic complexes that could provide synthetic analogs to WOC in PSII.

Supplementary Materials: The following supporting information can be downloaded at: https://www.mdpi.com/article/10.3390/chemistry5020049/s1, Electronic Supplementary Information file containing crystallographic details, bond valence sum calculations, and XPS spectra (Table S1. Crystallographic and data collection parameters for complexes **1** and **2**; Table S2. Bond Valence sum calculations for complexes **1** and **2**; Figure S1. XPS spectrum for complex **1**; Figure S2. XPS spectrum for complex **2**).

Author Contributions: Conceptualization, E.C.S.; methodology, E.C.S.; formal analysis, E.C.S.; experimental execution, J.B.B., K.C.N., and S.M.Q.; writing—original draft preparation, review, and editing, E.C.S.; supervision, E.C.S.; project administration, E.C.S.; funding acquisition, E.C.S. All authors have read and agreed to the published version of the manuscript.

Funding: This research was funded by Ministerio de Ciencia e Innovación, Spanish Government, grant number PGC2018-098630-B-I00.

Data Availability Statement: Data available upon request to corresponding author.

Conflicts of Interest: The authors declare no conflicts of interest.

References

1. Umena, Y.; Kawakami, K.; Shen, J.-R.; Kamiya, N. Crystal Structure of Oxygen-Evolving Photosystem II at a Resolution of 1.9 Å. *Nature* **2011**, *473*, 55–60. https://doi.org/10.1038/nature09913.
2. Suga, M.; Akita, F.; Hirata, K.; Ueno, G.; Murakami, H.; Nakajima, Y.; Shimizu, T.; Yamashita, K.; Yamamoto, M.; Ago, H.; et al. Native Structure of Photosystem II at 1.95 Å Resolution Viewed by Femtosecond X-Ray Pulses. *Nature* **2014**, *517*, 99–103. https://doi.org/10.1038/nature13991.
3. Suga, M.; Akita, F.; Sugahara, M.; Kubo, M.; Nakajima, Y.; Nakane, T.; Yamashita, K.; Umena, Y.; Nakabayashi, M.; Yamane, T.; et al. Light-Induced Structural Changes and the Site of O=O Bond Formation in PSII Caught by XFEL. *Nature* **2017**, *543*, 131–135. https://doi.org/10.1038/nature21400.

4. Gerey, B.; Gouré, E.; Fortage, J.; Pécaut, J.; Collomb, M.-N. Manganese-Calcium/Strontium Heterometallic Compounds and Their Relevance for the Oxygen-Evolving Center of Photosystem II. *Coord. Chem. Rev.* **2016**, *319*, 1–24. https://doi.org/10.1016/j.ccr.2016.04.002.
5. Arauzo, A.; Bartolomé, E.; Benniston, A.C.; Melnic, S.; Shova, S.; Luzón, J.; Alonso, P.J.; Barra, A. Slow Magnetic Relaxation in a Dimeric Mn_2Ca_2 Complex Enabled by the Large Mn (III) Rhombicity. *Dalton Trans.* **2017**, *46*, 720–732. https://doi.org/10.1039/c6dt02509a.
6. Kanady, J.S.; Tsui, E.Y.; Day, M.W.; Agapie, T. A Synthetic Model of the Mn_3Ca Subsite of the Oxygen-Evolving Complex in Photosystem II Jacob. *Science* **2011**, *333*, 733–736.
7. Tsui, E.Y.; Tran, R.; Yano, J.; Agapie, T. Redox-Inactive Metals Modulate the Reduction Potential in Heterometallic Manganese-Oxido Clusters. *Nat. Chem.* **2013**, *5*, 293–299. https://doi.org/10.1038/nchem.1578.
8. Kanady, J.S.; Lin, P.; Carsch, K.M.; Nielsen, R.J.; Takase, M.K.; Goddard, W.A.; Agapie, T. Toward Models for the Full Oxygen-Evolving Complex of Photosystem II by Ligand Coordination to Lower the Symmetry of the Mn_3CaO_4 Cubane: Demonstration That Electronic Effects Facilitate Binding of a Fifth Metal Jacob. *J. Am. Chem. Soc.* **2014**, *136*, 14373–14376.
9. Mukherjee, S.; Stull, J.A.; Yano, J.; Stamatatos, T.C.; Pringouri, K.; Stich, T.A.; Abboud, K.A.; Britt, R.D.; Yachandra, V.K.; Christou, G. Synthetic Model of the Asymmetric $[Mn_3CaO_4]$ Cubane Core of the Oxygen-Evolving Complex of Photosystem II. *Proc. Natl. Acad. Sci. USA* **2012**, *109*, 2257–2262. https://doi.org/10.1073/pnas.1115290109.
10. Zhang, C.; Chen, C.; Dong, H.; Shen, J.-R.; Dau, H.; Zhao, J. A Synthetic Mn_4Ca-Cluster Mimicking the Oxygen-Evolving Center of Photosynthesis. *Science* **2015**, *348*, 690–693.
11. Ledezma-Gairaud, M.; Pineda, L.W.; Aromí, G.; Sañudo, E.C. Microwave Assisted Synthesis: A Mn/Ni Reaction System Affording Mn_5Ni_4, Mn2Ni2 and Mn_7 Complexes. *Polyhedron* **2013**, *64*, 45–51. https://doi.org/10.1016/j.poly.2013.02.018.
12. Ledezma-Gairaud, M.; Grangel, L.; Aromí, G.; Fujisawa, T.; Yamaguchi, A.; Sumiyama, A.; Sañudo, E.C. From Serendipitous Assembly to Controlled Synthesis of 3d-4f Single-Molecule Magnets. *Inorg. Chem.* **2014**, *53*, 5878–5880. https://doi.org/10.1021/ic500418e.
13. Ledezma-Gairaud, M.; Pineda, L.W.; Aromí, G.; Sañudo, E.C. Synthesis and Characterization of New Mixed-Valent Mn(II)/Mn(III) and Mixed Metal Ni/Mn Complexes. *Inorg. Chim. Acta* **2015**, *434*, 215–220. https://doi.org/10.1016/j.ica.2015.05.030.
14. Milway, V.A.; Tuna, F.; Farrell, A.R.; Sharp, L.E.; Parsons, S.; Murrie, M. Directed Synthesis of $\{Mn_{18}Cu_6\}$ Heterometallic Complexes. *Angew. Chem.—Int. Ed.* **2013**, *52*, 1949–1952. https://doi.org/10.1002/anie.201208781.
15. Liu, W.; Thorp, H.H. Bond Valence Sum Analysis of Metal-Ligand Bond Lengths in Metalloenzymes and Model Complexes. 2. Refined Distances and Other Enzymes. *Inorg. Chem.* **1993**, *32*, 4102–4105.
16. Brown, I.D.; Altermatt, D. Bond-Valence Parameters Obtained from a Systematic Analysis of the Inorganic Crystal Structure Database. *Acta Cryst.* **1985**, *B41*, 244–247.
17. Brown, I.D.; Wu, K.K. Empirical Parameters for Calculating Cation–Oxygen Bond Valences. *Acta Cryst. B* **1976**, *32*, 1957–1959. https://doi.org/10.1107/S0567740876006869.
18. Chilton, N.F.; Anderson, R.P.; Turner, L.D.; Soncini, A.; Murray, K.S. PHI: A Powerful New Program for the Analysis of Anisotropic Monomeric and Exchange-Coupled Polynuclear d- and f-Block Complexes. *J. Comput. Chem.* **2013**, *34*, 1164–1175. https://doi.org/10.1002/jcc.23234.